Behaviors of the Spacers on the Galloping of Power Transmission Lines

Hwan-Seong KIM*, Tuong-Long NGUYEN* and Gi-Sig BYUN**
* Department of Logistics Engineering, Korea Maritime University, Pusan, KOREA
(Tel: +82-51-410-4334; E-mail: kimhs@kmaritime.ac.kr)
(Tel: +82-51-410-4914; E-mail: longnguyen@gmx.de)
** Department of Control & Instrumentation Engineering, Pukyong National University, Pusan, KOREA
(Tel: +82-51-620-1634; E-mail: gsbyun@pknu.ac.kr)

Abstract: In this paper, we have proposed a method by using virtual simulation to calculate the behaviors of spacers to avoid conductor galloping with the hanging composite polymer spacer between conductors on different phases. We have considered with three types of modeling considerations for the analysis of galloping in power transmission lines, such as iced-single conductors without spacer, iced-single conductors with spacers, and iced-two bundle conductors with spacers. In simulation, the finite element method is used to calculate the structural response with geometric nonlinear behavior. The iced conductor is modeled by two beam-element faces with which it is connected. The ANSYS program is applied too. First, the calculation results show that the two beam-element model is very suitable to make a virtual simulation. Second, the amplitude of conductor galloping is reduced after hanged spacers. Third, when number of spacer is increased, the maximum magnitude of natural frequency of iced conductor will reduce. Final, the behaviors of spacers are verified in viewpoint of standard cases.

Keywords: Power Transmission Line, Finite Element Method, Identification

1. INTRODUCTION

The power transmission systems in South Korea are 66 kV, 154 kV and 345 kV. Their purpose is to bring electricity from the power stations to the center of large cities and to the factories. Especially, 154 kV transmission line is constructed between Seoul and Pyong Yang in 1935. In the future, transmission planning is divided into three categories: long-mid-short-term. The mid-term and the short-term plan are the expansion of system facilities of 154 kV during the next time. And also, we need to make the hanging composite polymer spacer between conductors on different phase with standard phase-to-phase distance. Generally, the hanging composite polymer spacer will be affecting the vibration of power transmission line (PTL). Besides, the conductor and iced conductor are subjected to wind flow; it may increase vibration or suddenly deflect its motion in wind flow around. Because of their motion, the cables from two different phases can come too close one from each other, therefore creating repeated short-circuits. Moreover, their motion may cause extensive damage to components of the conductor with support system or to the conductor itself.

Generally, this kind of situation can be called as “galloping”. Galloping is the name used for aerodynamic and aero elastic instabilities on overhead line conductor. It is the instability typical of slender structures. Galloping of iced conductors has been a design and operating problem since early 1920's. Especially, low frequency (from 0.15 Hz to 1 Hz) and high amplitude galloping of the conductor is a serious problem in the overhead power transmission line conductor [1]-[3].

Over the years considerable effect has been made to identify the galloping mechanisms and to find a solution to this problem. In the last time, many models have been developed in order to simulate galloping and try to understand it better. By using mechanical devices, some authors develop many methods to avoid galloping such as hanging composite polymer spacer, pendulum detuners, windamper, twister, torsional damper detuner (TDD), etc.. [4]-[9].

Generally, there are two kinds of simulations such as simulation with experiment based on real test conducted lines and simulation with just numerical computing. In numerical simulation, there are two cases: linear/non-linear differential equations and finite element modeling method.

In this paper, the experiments conducted on test lines are not determined, so process by simulation is predicted virtual simulation on computer. We have proposed a method by using virtual simulation to calculate the behaviors of spacers to avoid conductor galloping with the hanging composite polymer spacer between conductors on different phases. We have considered with three types of modeling considerations for the analysis of galloping in power transmission lines, such as iced-single conductors without spacer, iced- single conductors with spacers, and iced - two bundle conductors with spacers. In simulation, the finite element method is used to calculate the structural response with geometric nonlinear behavior. The iced conductor is modeled by two beam-element faces with which it is connected. The ANSYS program is applied too [10]-[12]. First, the calculation results show that the two beam-element model is very suitable to make a virtual simulation. Second, the amplitude of conductor galloping is reduced after hanged spacers. Third, when number of spacer is increased, the maximum magnitude of natural frequency of iced conductor will reduce. Final, the behaviors of spacers are verified in viewpoint of standard cases.

2. CONSIDERATIONS

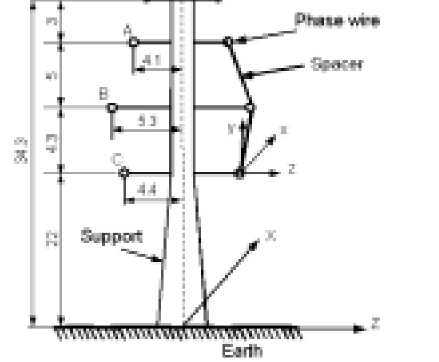

Fig. 1 Characteristics of PTL and Spacer.

In this paper, we assume the following 154 kV overhead power transmission line with inter-phase spacer (hanging composite polymer spacer) in Fig.1. In 154 kV overhead power transmission line, generally an aluminum conductor steel reinforced (ACSR) type is used. ACSR electrical conductor, called darke 2617 (with 26 aluminum wires and 7 steel wires) was used in whole of this paper. And also, the tower sketch is used by the standard phase-to-phase distance ($4.3[m]$ and $5[m]$).

3. VIRTUAL SIMULATION

A virtual simulation system can simulate the properties of the real models. Virtual simulation of spacers to avoid conductor galloping replaces the real simulation with a virtual models. Virtual simulation provides more cases than a real simulation in order to try to understand it better.

3.1 Parameters of model for Simulation

3.1.1 The level Catenary

A span of Drake conductor with ends at the same clevation is shown in Fig. 2. And, the catenary has an equation of the form

$$y = \frac{H}{m}\left[\cosh(\frac{m}{H}x) - 1\right] \tag{1}$$

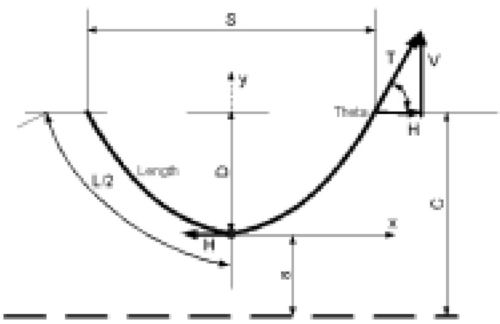

Fig. 2 The Level Catenary.

Table 1 Parameters of Model for Simulation.

Symbols	Values	Units
Tension (H)	25742.2145	$[N]$
Acceleration of gravity (g)	9.81	$[m/s^2]$
Span (S)	350	$[m]$
Sag (D)	9.5	$[m]$
Mass of conductor (m)	1.628	$[m]$
Curvature coefficient (a)	1611.842	$[kg/m]$
Angle of attachment (θ)	6.21172	$[Deg]$
Length (L)	6.21172	$[m]$
Tension (T)	25894.1	$[N]$

3.1.2 Diameter of iced conductor

The movements of iced conductor are reacted by the forces on the each axes and by the moments on each rotation angles, and these kind force and moment are generated by wind force. Normally, the magnitude of forces and moments depend on the velocity of wind and the angle of wind attack. Fig. 3 denotes the definitions of the forces and shows the relation between wind forces, lift and drag forces.

Ice has been chosen close to Tunstall's shape and adapted to the outside diameter of the conductor, (artificial ice - silicone: density is $1.1-1.5[g/cm^3]$, tensile strength is $6.5[MPa]$.

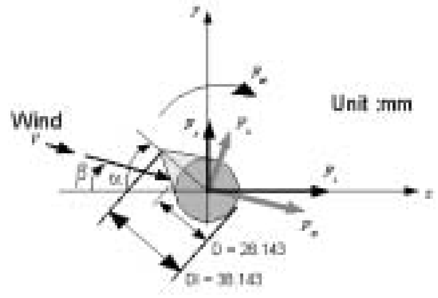

Fig. 3 Wind Attack Forces and Icing Angle.

where, α denotes icing angle, β is angle of wind attack, V denotes a wind velocity, F_L and F_D represent lift force and drag force, respectively.
These forces F_L, F_D and movement F_M are given as

$$F_D = \frac{1}{2}C_D\rho v^2 s \tag{2}$$

$$F_L = \frac{1}{2}C_L\rho v^2 s \tag{3}$$

$$F_M = \frac{1}{2}C_M\rho v^2 s D_{IC} \tag{4}$$

where C_L is coefficient of lift force, C_D is coefficient of drag force, ρ is mass density of air, D is diameter of conductor, and S is area acting wind force. D_{IC} is diameter of conductor and ice.

By considering the angle of wind attack, the forces on y and z axes are given as

$$F_z = F_D cos\beta + F_L \sin\beta \tag{5}$$

$$F_y = F_L cos\beta - F_D \sin\beta \tag{6}$$

Generally, the lift and drag forces depends on the icing shape, ice size, and icing angle etc.. For simulation of galloping, the data for lift, drag forces and moment are necessary. In this paper, we use a result [5] which obtained by wind tunnel test as in Fig. 4.

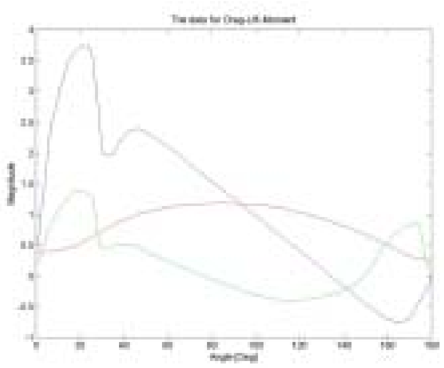

Fig. 4 Aerodynamic characteristics.

3.2 Virtual Simulation

3.2.1 Based Model

The based model is shown in Fig. 5. This model is used by two beam4-elements. Finite element analysis is based on adiscrete representation of continuous behaviour. Each objects divided into a mesh of beam elements connected at nodes.

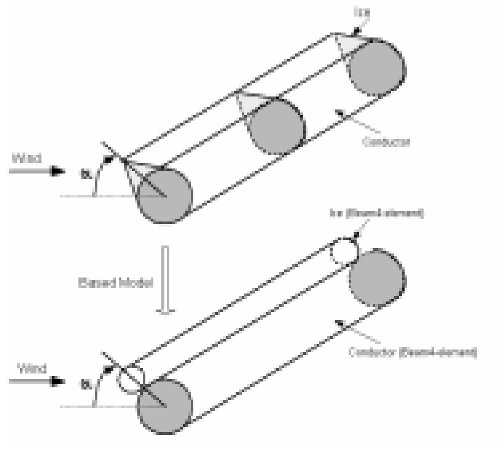

Fig. 5 Based Model.

Based model is two beam-element faces with which it is connected. For structural analyses, a list of nodes is defined along with the nodal directions in which these nodes are to be coupled. As a result of this coupling, these nodes are forced to take the same displacement in the specified nodal coordinate direction. The amount of the displacement is unknown until the analysis is completed. All other degrees of freedom in the coupled sets are eliminated from the solution matrices by their relationship to the prime degree of freedom. Forces applied to coupled nodes (in the coupled degree of freedom direction) will be summed and applied to the prime degree of freedom. Output forces are also summed at the prime degree of freedom.

The fundamental equation of any dynamic model of a system can be described by differential equation of linear dynamic elasticity.

$$M\ddot{x} + D\dot{x} + Kx = F \qquad (7)$$

where M, D, and K denote the global mass, damping and global stiffness matrices, respectively. Also F is the load v ector of forces acting on the nodes. And x is the vector o f nodal displacements.

The basic algorithm of the block Lanczos method [10] is used to determine the natural frequency of models. This method uses the sparse matrix solver.

The nonlinear static analysis [11]-[12] is used to determine the displacement, stress, bending moment of models.

The finite element method (ANSYS program) is used to determine the structural response of PTL. Beam4-element is applied for models.

3.2.2 Matrices

The element stiffness matrix

The element stiffness matrix k_l in element coordinates is given as

$$[k_l] = \begin{bmatrix}
\frac{AE}{L} & & & & & & & & & & & \\
0 & a_z & & & & & & & & & & \\
0 & 0 & a_y & & & & & & & & & \\
0 & 0 & 0 & \frac{GJ}{L} & & & & & \mathit{Symmtric} & & & \\
0 & 0 & -c_y & 0 & e_y & & & & & & & \\
0 & c_z & 0 & 0 & 0 & e_z & & & & & & \\
\frac{-AE}{L} & 0 & 0 & 0 & 0 & 0 & \frac{AE}{L} & & & & & \\
0 & -a_z & 0 & 0 & 0 & -c_z & 0 & a_z & & & & \\
0 & 0 & -a_y & 0 & c_y & 0 & 0 & 0 & a_y & & & \\
0 & 0 & 0 & -\frac{GJ}{L} & 0 & 0 & 0 & 0 & 0 & \frac{GJ}{L} & & \\
0 & 0 & -c_y & 0 & f_y & 0 & 0 & 0 & c_y & 0 & e_y & \\
0 & c_z & 0 & 0 & 0 & f_z & 0 & -c_z & 0 & 0 & 0 & e_z
\end{bmatrix} \qquad (8)$$

where A, E, L, G and J denote cross section area, Young's modulus, element length, shear modulus and torsional moment of inertia, respectively. And

$$J = \begin{cases} J_x & if \quad I_x = 0 \\ I_x & if \quad I_x \neq 0 \end{cases}$$

where I_x and J_x denote torsional moment of inertia. the polar moment of inertia has relationship as

$$J_x = I_y + I_z$$

with

$$a_z = a(I_z, \varphi_y)$$
$$a_y = a(I_y, \varphi_z)$$
$$b_z = a(I_z, \varphi_y)$$
$$f_z = f(I_z, \varphi_y)$$
$$f_y = f(I_y, \varphi_z)$$

The element mass matrix

The element mass matrix $[M_l]$ in element coordinates is considered as (without lumped mass)

$$[M_l] = M_t \times \begin{bmatrix}
\frac{1}{3} & & & & & & & & & & & \\
0 & A_z & & & & & & & & & & \\
0 & 0 & A_y & & & & & & & & & \\
0 & 0 & 0 & \frac{J_x}{3A} & & & & & \mathit{Symmtric} & & & \\
0 & 0 & -C_y & 0 & E_y & & & & & & & \\
0 & C_z & 0 & 0 & 0 & E_z & & & & & & \\
\frac{1}{6} & 0 & 0 & 0 & 0 & 0 & \frac{1}{3} & & & & & \\
0 & B_z & 0 & 0 & 0 & D_z & 0 & A_z & & & & \\
0 & 0 & B_y & 0 & -D_y & 0 & 0 & 0 & A_y & & & \\
0 & 0 & 0 & \frac{J_x}{6A} & 0 & 0 & 0 & 0 & 0 & \frac{J_x}{3A} & & \\
0 & 0 & D_y & 0 & F_y & 0 & 0 & 0 & -C_y & 0 & E_y & \\
0 & -D_z & 0 & 0 & 0 & F_z & 0 & C_z & 0 & 0 & 0 & E_z
\end{bmatrix} \qquad (9)$$

where

$$M_t = (\rho A + m)\, L\, (1 - \varepsilon^{in})$$

ρ, m and ε^{in} denote density, added mass per unit length and prestrain, respectively.

with

$A_z = A(r_z, \varphi_y)$; $A_y = A(r_y, \varphi_z)$; $B_z = A(r_z, \varphi_y)$;

$F_z = F(r_z, \varphi_y)$; $F_y = F(r_y, \varphi_z)$.

Stress Calculations

$$\sigma_i^{dir} = \frac{F_{x,i}}{A} \tag{10}$$

where σ_i^{dir} and $F_{x,i}$ denote centroidal stress and axial force, respectively.

The bending stresses

$$\sigma_{z,i}^{bnd} = \frac{M_{y,i} t_z}{2I_y} \tag{11}$$

where $\sigma_{z,i}^{bnd}$ denotes bending stress in element x direction on the element $+z$ side of the beam at end i.

$$\sigma_{y,i}^{bnd} = \frac{M_{z,i} t_y}{2I_z} \tag{12}$$

where $\sigma_{y,i}^{bnd}$ denotes bending stress in element x direction on the element $-y$ side of the beam at end i. And $M_{y,i}$, $M_{z,i}$ denote moment about the element y axis at end i, denote moment about the element z axis at end i

And t_z, t_y denote thickness of beam in element z direction, denote thickness of beam in element y direction, respectively.

The maximum and minimum stresses

$$\sigma_i^{\max} = \sigma_i^{dir} + \left|\sigma_{z,i}^{bnd}\right| - \left|\sigma_{y,i}^{bnd}\right| \tag{13}$$

$$\sigma_i^{\min} = \sigma_i^{dir} - \left|\sigma_{z,i}^{bnd}\right| - \left|\sigma_{y,i}^{bnd}\right| \tag{14}$$

4. A SIMULATION RESULTS

We considered with three types of modeling for the analysis of galloping in PTL such as iced-single conductor without spacer, iced- single conductor with spacers, and iced- 2 bundle conductors with spacers.

4.1 The iced-single conductors without spacer

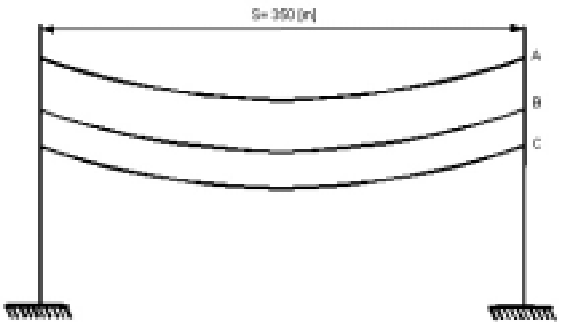

Fig. 6 Model of Iced-Single Conductors without Spacer.

4.1.1 Finding natural frequency and its magnitude

Table 2 Maximum Magnitudes

Mode	Maximum magnitude $[m]$	Natural frequency $[Hz]$
1	0.065459	0.015179
2	0.064739	0.41992
3	0.063232	0.94026

Table 3 Maximum Rotation

Mode	Maximum rotation [deg]	Natural frequency $[Hz]$
1	0.058192	2.553
2	0.056284	2.4608
3	0.056284	2.4608

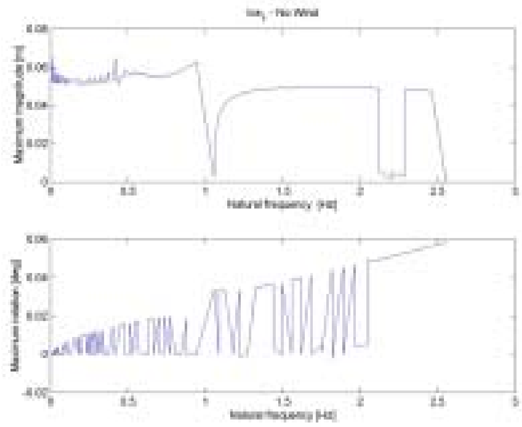

Fig. 7 Maximum Magnitude and Maximum Rotation.

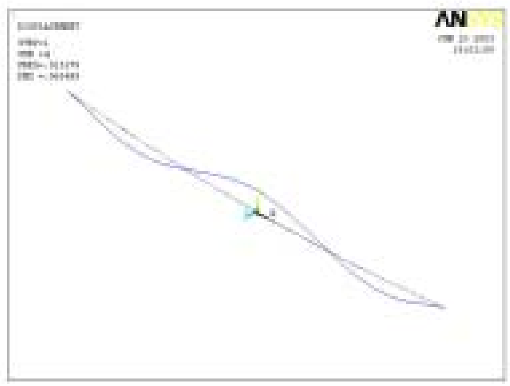

Fig. 8 Mode Shape.

4.1.2 Finding Maximum Jumping distance (center point)

We take a initial parameters of iced conductor as, initial angle of icing is $\alpha = 40^0$, initial angle of wind attack $\beta = 30^0$.

By considering the general analysis procedures in Fig. 9, we obtain the maximum jumping distance and angle of iced-single conductor as $13.698[m]$ and $3.413[rad]$, with the velocity is $10[m/s]$.

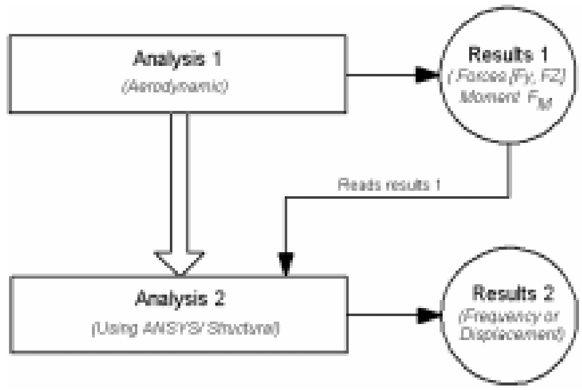

Fig. 9 Analysis Procedure

4.2 Single and two bundle conductors with spacers

We can find the maximum compression or tension of spacers and maximum bending moment of spacers. We considered three conductors with 4 cases as in Fig.10. The velocity is $10\,[m/s]$.

In this section, we used Beam4-element with $6\,DOF$. For instance, when the span $S = 350\,[m]$, the spacers is hanged in the position away $L/3$ from suspension point. In the future, we change the length of span $(S > 350 \text{ or } S < 350)$. And, we have to get a good database for aerodynamic curves (drag, lift and moment) from very thin to thick typical ice accretion. The based models will include suspension (torsional stiffness).

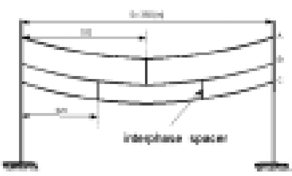

Case 1

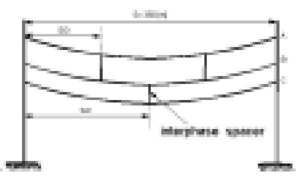

Case 2

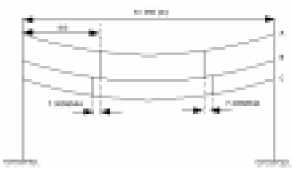

Case 3

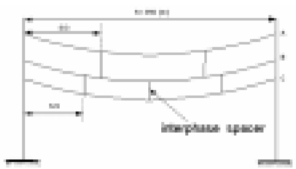

Case 4

Fig. 10 The Position of Three Phases Conductors and Spacers

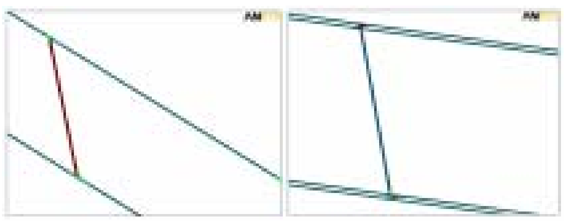

Fig. 11 Single and two Bundles PTL with Spacers

4.2.1 Results for iced conductor

The maximum magnitude and maximum rotation of models at the first natural frequency are shown in Table 4.

Table 4 Magnitude and Rotation

Models		No spacer	Case1	Case2	Case3	Case4
Single PTL with spacer	Mag.	0.0654	0.0647	0.0595	0.0573	0.0614
	Rot.	0.0581	0.0163	0.0147	0.0100	0.0210
2 bundle PTL with spacers	Mag.	0.0654	0.0517	0.0512	0.0652	0.0499
	Rot.	0.0581	0.0084	0.0037	0.0063	0.0128

4.2.2 Results for spacers

The flexible spacers are considered too, with material properties: diameter of spacer is $\phi = 40\,[mm]$, elastic modulus is $E = 41\,[kN/mm^2]$, and density is $0.073\,[Lbs/in^3]$. The element coordinate system of spacers is shown in Fig. 12.

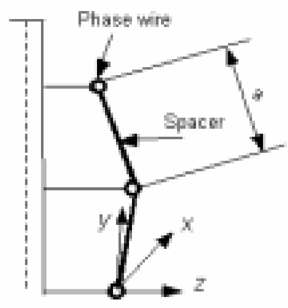

Fig. 12 Element Coordinate System of Spacers.

Table 5 Tension and axial direct stress of spacer

Models		Case1	Case2	Case3	Case4
Single PLT with spacer	Tension	2.048	1.626	2.071	1.766
	Stress	1630	1294	1648	1405
2 bundle PLT with spacer	Tension	2.526	2.622	2.526	2.232
	Stress	2010	2112	2010	1776

Table 6 Maximum Bending Moment of Spacers

Models		Case1	Case2	Case3	Case4
Single PTL with spacers	*Mx*	0.3079	0.1889	1.985	0.3540
	My	23.919	36.367	24.523	18.619
	Mz	72.855	42.828	89.375	109.168
2 bundle PTL with spacers	*Mx*	0.007	0.060	0.078	0.059
	My	34.865	47.183	35.123	31.152
	Mz	3.567	4.066	4.076	4.843

The calculation results show that the bending moment ($Mz\,[N.m]$) of spacers in single PTL is max. as Fig. 13.

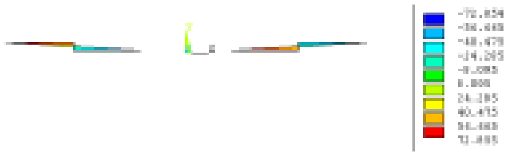

Fig. 13 Single PTL with Spacers (Case1).

Also, the calculation results show that the bending moment ($My\,[N.m]$) of spacers in 2- bundles PTL is max. as Fig. 14.

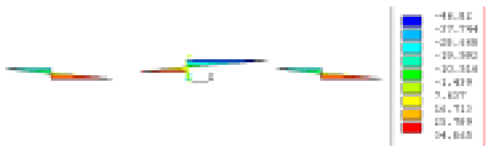

Fig. 14 Two Bundles PTL with Spacers (Case1).

5. CONCLUSION

We have proposed a method by using virtual simulation to calculate the behaviors of spacers to avoid conductor galloping with the hanging composite polymer spacer between conductors on different phases. We have considered with three types of modeling considerations for the analysis of galloping in power transmission lines, such as iced-single conductors without spacer, iced-single conductors with spacers, and iced-two bundle conductors with spacers. First, the calculation results show that the two beam-element model is very suitable to make a virtual simulation. Second, the amplitude of conductor galloping is reduced after hanged spacers. Third, when number of spacer is increased, the maximum magnitude of natural frequency of iced conductor will reduce. Final, the behaviors of spacers are verified in viewpoint of standard cases. In the future, how to insert the hanging composite polymer spacer between conductors on different phase with standard phase-to-phase distance which influences other element is a more important problem. Therefore, there needs a lot of computational time compare with other methods.

REFERENCES

[1] J.P. Den Hartog, "Transmission Line Vibration Due to Sleet", Transactions AIEE, Vol. 51, No. 12, pp. 1074-086, 1932.

[2] E. Simiu and R.H. Scanlan, "Wind effects on structures -Fundamentals and Applications to Design", Third Edition, John Wiley and Sons, 1996.

[3] K. Goto and T. Koike, "A Numerical Calculation Method for Galloping and Prevention of it", The Japan Institute of Electrical Engineers, No. 7, 1977.

[4] C.J. Noh, H.S. Park and G.S. Byun, "The Analysis of Power Line Galloping by Describing Function Method', The Korean Institute of Electrical Engineers, Vol. 41, No. 4, pp. 339-345, 1992.

[5] H.S. Kim and G.S. Byun "A Atudy on The Analysis of Galloping for Power Transmission Line", ISIE, Pusan, Korea, pp. 973-978, 2001.

[6] H. S. Kim, T. L. Nguyen and G. S. Byun, "A Coupled-Field Analysis of Galloping for Power Transmission Line", ICCAS 2002, International Conference on Control, Automation and Systems, Muju Resort, Jeonbuk, Korea, 2002.

[7] Liming Wang, Yu Yin, Xidong Liang, Zhicheng Guan, "Study on air insulator strength under conductor galloping condition by phase to phase", Annual report conference on Electrical Insulation and Dielectric Phenomena, Department of Electrical, Tsinghua University, China, pp. 617-619, 2001.

[8] M. Tunstall and L.T. Kotselos, "Further Studies of The Galloping Instability of Natural ice Accretion on Overhead Line Conductors", Atmospheric Icing of Structures, Paris, 1988.

[9] R. Keutgen and J.L. Lilien, "Benchmark Cases for Galloping with Results Obtained from Wind Tunnel Facilities-Validation of a Finite Element Model", IEEE Vol. 15, No. 1, 2000.

[10] Grimes, R. G. Lewis, J. G., Simon, H. D., "A shifted block Lanczos algorithm for solving sparse symmetric generalized eigenproblems, SIAM J. Matrix Anal. Appl, V. 15, pp. 1-45, 1994.

[11] P.C. Kohnke, "ANSYS Engineering Analysis System Theoretical Manual", Swanson analysis system, Inc., Houstom, PA, 1989.

[12] G. Poole, Y.C. Liu, J. Mandel, "Advancing Analysis Capabilities in ANSYS Through Solver Technology", ANSYS, Inc., Canonsburg, 2001.